Available online at www.sciencedirect.com
SCIENCE DIRECT®
Journal of Sound and Vibration 282 (2005) 769–780
JOURNAL OF SOUND AND VIBRATION
www.elsevier.com/locate/jsvi

# Amplitude–frequency dependence of damping properties of carbon foams

Konstantin Maslov*, Vikram K. Kinra

*Department of Aerospace Engineering, Texas A&M University, College Station, TX 77843-3141, USA*

Received 8 August 2003; accepted 13 March 2004
Available online 28 October 2004

**Abstract**

Wide dynamic and frequency range experimental measurements of dynamic shear modulus and specific damping capacity in carbon foams are presented. Samples have been placed in free vibration mounts, in vacuum. Electromagnetic excitation and optical detection of free vibration decay have been used. Elastic modulus and loss factor have been inverted from resonance frequencies and logarithmic decay measurement performed at several (up to ten) normal-mode resonances using a modified Demarest's theory of cube resonance. For the samples under investigation, the dynamic shear modulus was found to be proportional to sample density and equal to 1 GPa for 0.5 kg/m$^3$. The specific damping capacity was found to be frequency independent in the 100 Hz–20 kHz frequency range and equal to 0.004 for 0.3 kg/m$^3$ foam samples and 0.012 for 0.5 kg/m$^3$ foam samples. Such behaviour cannot be explained by the difference in foam structure and must be caused by a difference in properties of the constitutive material. The specific damping capacity increases more than twice with increase in magnitude of material deformation. Technical problems, such as the contribution of parasitic damping to the loss factor, are discussed in detail.


## 1. Introduction

Carbon foams, a new class of foamed materials, have been introduced recently [1]. Carbon foams are inexpensive, lightweight (with densities around $0.3 \times 10^3$ kg/m$^3$), fire resistant and impact absorbing. They also possess good three-dimensional isotropic strength characteristics,

*Corresponding author. Tel.: +1-979-862-7662; fax: +1-979-845-6051.
*E-mail address:* kinra@aero.tamu.edu (K. Maslov).

0022-460X/$ - see front matter © 2004 Elsevier Ltd. All rights reserved.
doi:10.1016/j.jsv.2004.03.041

highly uniform micro-cellular distribution, and are able to operate at higher temperatures [2]. They are currently being evaluated for a variety of applications such as aerospace thermal management systems, impact mitigation for aircraft and as core material in aerospace sandwich structures. For many such applications, damping properties of the material are of great importance. A high damping capacity expressed by a high loss factor is usually desired [3,4].

While the real (pure elastic) part of the elastic moduli of porous materials can be easily found using static measurements [5], measuring the loss factor of foam is a non-trivial task. To the best of our knowledge, there are no works reporting damping properties of carbon foams. However, from the viewpoint of measurement techniques, carbon foams might be compared to aluminium foams, the damping measurements for which were discussed elsewhere in detail [3,4]. Most accurate up-to-date damping measurements in aluminium foams were performed by a resonance technique using the cantilevered beam mount [3], yielding measurements accuracy of about 40% for low density (80% porosity) foams. A high level of additional friction in the cantilever beam mount reportedly caused this rather low accuracy. However, measurements using a simply suspended free-vibrating sample were even less repeatable due to high losses at the rigid support caused by the difficulty of locating the vibration nodes in an inhomogeneous foam sample.

In case of carbon foam, which has low brittle-fracture toughness, the clamping problem becomes overwhelmingly difficult and the free-resonance technique has to be reconsidered. Support losses could be minimized by using very thin and flexible supporting wire, providing that vibration detection (and excitation) is insensitive to the equilibrium sample position in space.

To perform measurements at high frequency, samples of near-cubic (not exactly cubic to avoid resonance overlapping) shape are used. At lower resonance frequencies typical for technical applications, flexure and torsion modes in samples shaped as long thin beams or plates are used [3,4]. In the case of foam material, minimum sample dimensions must be much larger than pore size; otherwise, statistical variations of sample porosity might cause irreproducible and meaningless results. To lower normal-mode resonance frequencies, samples of a more complex shape such as the tuning fork can be used. Moreover, by using equal but oppositely directed excitation forces applied to opposite fork legs it becomes possible to excite high (up to ultimate sample strength) vibration amplitude and perform wide dynamic range measurements, thus overcoming one of the major complains about the practical insignificance of resonance (acoustic) measurements, those addressing the extremely small level of deformations at which measurements are usually taken compared to what the material under test meets in practical application.

Development of a robust inversion procedure for complex elastic constants of foams, and measurements of the specific damping capacity of newly developed carbon foams are the main goals of the present article.

## 2. Theory

It is reasonable to expect that normal-mode resonance frequencies, which are controlled by a complex elastic tensor, material density and size and shape of the samples, can be used to measure the elastic moduli and the correspondent loss factors of the material [6]. The inverse problem, that is calculation of material properties from the measured normal-mode resonance properties, can be solved by minimizing the difference between measured and calculated resonance frequencies and/

or quality factors in a least-square sense. The minimization procedure necessarily requires repetitive calculations of resonance frequencies, and the calculation scheme must therefore be simplified as much as possible. However, with a few exceptions, the analytical solution for frequencies of normal modes has not been found, and numerical techniques must be used.

In practice, finite element numerical [7], and approximate semi-analytical methods have been developed [6,8]. Demarest's [9] variational approach is used here because it results in a simple linear matrix equation, which greatly simplifies inversion of material parameters from experimental data. Ohno and others [10,11] have refined this method and its application to the determination of elastic constants of materials, and have shown that complex elastic constants, and thus material damping properties, can also be measured using this method [11].

According to Refs. [6,9–11] the motion, $\mathbf{u}(\mathbf{x}_i)\exp(\mathrm{i}\omega t)$, of an isolated pure elastic object of an arbitrary shape and volume $V$ is given by a displacement function $\mathbf{u}(\mathbf{x}_i)$ that renders the Lagrangian $L$ stationary, i.e.

$$\delta L = \delta \int_V (\text{kinetic energy-potential energy})\,\mathrm{d}V = \tfrac{1}{2}\delta \int_V (\rho\omega^2 \mathbf{u}_i\mathbf{u}_j - \mathbf{C}_{ijkl}\mathbf{u}_{i,j}\mathbf{u}_{k,l})\,\mathrm{d}V = 0, \quad (1)$$

where an index after a comma represents partial derivative. To solve Eq. (1) the displacement function is expressed in a series

$$\mathbf{u}_i = \mathbf{a}_{i\xi}\mathbf{\Phi}_\xi, \quad (2)$$

where $\mathbf{\Phi}_\xi = \mathbf{\Phi}_m(x_1)\cdot\mathbf{\Phi}_p(x_2)\cdot\mathbf{\Phi}_q(x_3)\cdot\mathbf{e}_i$ is a set of basis functions, $\mathbf{e}_i$ is a unit vector in $\mathbf{x}_i$ direction, $\xi = (i,m,p,q)$ is the function label—a non-negative integer, and the $\mathbf{a}_{i\xi}$ are unknown coefficients that define the mode shape at resonance frequency $\boldsymbol{\omega}_n = 2\pi\mathbf{f}_n$. Substituting Eq. (2) into Eq. (1) gives the generalized eigenvector equation to determine $\mathbf{a}_{i\xi}$,

$$\mathbf{a}_{\xi i}\left(\omega^2\boldsymbol{\delta}_{ij}\int_V \rho\mathbf{\Phi}_\xi\mathbf{\Phi}_{\xi'}\,\mathrm{d}V - \int_V \mathbf{\Phi}_{\xi,k}\mathbf{C}_{ijkl}\mathbf{\Phi}_{\xi',l}\,\mathrm{d}V\right)\cdot\mathbf{a}_{j\xi'} = 0, \quad (3)$$

where $\boldsymbol{\delta}_{ij}$ is Kronecker delta function.

In order to solve Eq. (3), the number of matrix elements must be truncated to a certain number. The approximate theory [6] does not have an exact criterion of resulting error. Typically, a set of basis functions is truncated at a point when the result becomes independent of matrix rank within chosen bounds.

Depending on material anisotropy only some of the elements of the elastic tensor in Eq. (3) are independent; others can be expressed as a linear combination of a few independent material parameters (for example, Lame constants for an isotropic solid) sequentially numbered here as $\mathbf{C}_r$. Correspondingly, resonance frequencies (and coefficients of series decomposition in Eq. (2)) become a solution to the generalized eigenvector problem

$$[\pi^2\mathbf{f}_n^2, \mathbf{a}_{i\xi}] = \mathrm{eig}\left(\rho\boldsymbol{\delta}_{ij}\int_V \mathbf{\Phi}_\xi\mathbf{\Phi}_{\xi'}\,\mathrm{d}V,\ \sum_r C_r\int_V \mathbf{\Phi}_{\xi,k}\mathbf{C}^{(r)}_{ijkl}\mathbf{\Phi}_{\xi',l}\,\mathrm{d}V\right), \quad (4)$$

where $\mathbf{C}^{(r)}_{ijkl}$ is a stiffness matrix in which all elements except coefficients at corresponding $\mathbf{C}_r$ are set to be equal to zero and the rest is normalized on $\mathbf{C}_r$. Knowing the forward solution for $\mathbf{f}_n(\rho,\mathbf{C}_r)$, the independent elastic constants $\mathbf{C}_r$ can be found using any suitable minimization

procedure, such as the Nelder–Mead simplex method with merit function

$$\mathrm{Err} = \sum_N (1 - f_N(\mathbf{C}_r)/f_N^{(e)})^2, \tag{5}$$

where the upper index $(e)$ designates experimentally measured quantities. Because matrix coefficients in Eq. (4) are calculated only one time in advance to the minimization procedure, the merit function calculation consists of a few algebraic manipulations, a matrix summation and an eigenvalue routine. This procedure is quite robust. It takes a few minutes on a 2 GHz personal computer to invert $\lambda$ and $\mu$ from experimental data even for an extremely large matrix (rank $\sim 10^3$).

There is no theory available to determine the best set of basis functions for a given sample shape. For a rectangular body (the sample shape used in these experiments) it has been shown that from the computational viewpoint the best choice for the basis functions are normalized Legendre polynomials [9–11]. Explicit expressions for Eq. (3) in algebraic form are given in Ref. [10]. Another set of basis functions better suited for objects whose shape is defined by second-order algebraic functions are Taylor series [6].

For more complex sample geometries, solution (4) converges very slowly, and use of large matrixes is required to get desired precision, which in turn faces the problem of numerical stability of the eigenvector routine. A tuning fork is a good example of such a shape. Very approximately, fork legs can be treated as separate Bernoulli beams. Correspondingly, their motion from and toward each other ($\boldsymbol{x}_2$-direction in Fig. 3) as a first approximation is independent of the $\boldsymbol{x}_2$-coordinate. Such a function does not exist in basis sets and a combination of higher-order basis functions has to make up its absence.

The solution can be significantly improved by artificially adding this zero-order solution to the set of basis functions. (This can be viewed as a variant of the successive approximation approach.) For a tuning fork made from a rectangular piece by machining a cut on one side between $-x_{20}$ and $x_{20}$ to the depth $x_{10}$, it adds a new (first) term in factor $\Phi_p(x_2)$, which is a negative constant for $x_2 < -x_{20}$, a positive constant for $x_2 > x_{20}$, and is smooth up to the second derivative everywhere. The simplest of such functions is

$$\Phi_0(x_2) = \begin{cases} -1 \\ \frac{3}{8x_{20}^5}x_2^5 - \frac{5}{4x_{20}^3}x_2^3 + \frac{15}{8x_{20}}x_2 \\ 1 \end{cases} \quad \text{at} \quad \begin{cases} x_2 < -x_{20}, \\ -x_{20} < x_2 < x_{20}, \\ x_2 > x_{20}. \end{cases} \tag{6}$$

Convergence of a solution (resonance frequency as a function of Legendre polynomial order) for the modified set of basis function as compared to the original set of Legendre polynomials is shown in Table 1. The experimentally measured resonance frequency is 238.5 Hz. As one can see, the standard solution gives 10% error at polynomial order 23 (matrix rank 1380), while using a modified basis function set the same result is attainable at polynomial order 11 (matrix rank 194), and starting with polynomial order 19, the result converges within 1%.

For an elastic body with low internal material damping, complex resonance frequencies $f_N^* = f_N(1 + \mathrm{i}(q_N/2))$ which are functions of complex elastic constants $C_R(1 + \mathrm{i}Q_R^{-1})$, and material

Table 1
Frequency of the first flexure mode of a tuning fork for different polynomial order

| Polynomial order | 9 | 11 | 13 | 15 | 17 | 19 | 21 | 23 | 25 | 27 | 29 |
|---|---|---|---|---|---|---|---|---|---|---|---|
| Legendre polynomial | 7049 | 4291 | 2521 | 1461 | 839 | 501 | 338 | 262 | 249 | 241 | 236 |
| Additional term in $P_p$ | 381 | 259 | 256 | 247 | 244 | 242 | 241 | 240 | 239 | 238 | 237 |

density, $\rho$, (no summation is assumed over indexes expressed by capital letters) can be introduced. Logarithmic decrements $q_N$ are measurable parameters that can be used to invert elastic constants of the material and measure its internal damping conjugate to the elastic constants, $Q_R^{-1}$. If $Q_R^{-1} \ll 1$, then the imaginary part of the elastic tensor can be considered as a small perturbation of it. Correspondingly, expanding $f_N(C_R, \rho)$ near the true value of $C_R$ and keeping only first-order terms, the relationship between experimentally measured quantities and material parameters can be expressed as

$$f_N^{(e)}\left(1 + \mathrm{i}\,\frac{q_N}{2}\right) \approx f_N^{(\mathrm{true})} + \sum_R (\partial f_N/\partial C_R)(\delta(C_R) + \mathrm{i}C_R Q_R^{-1}), \tag{7}$$

where $\delta(C_R)$ are errors in measurements of the elastic constant $C_R$. Internal material damping $Q_R^{-1}$ is inverted from the imaginary part of Eq. (7) as

$$\mathbf{Q}_r^{-1} = (\mathbf{S}_{rp}\mathbf{S}_{pm})^{-1}\mathbf{S}_{mn}\frac{\mathbf{q}_n}{2}, \tag{8}$$

where

$$S_{NR} = \frac{\partial f_N/\partial C_R}{f_N/C_R} \tag{9}$$

are sensitivities of measurable quantities $q_N/2$ and $f_R^{(e)}$ to the material parameters $Q_R^{-1}$ and $C_R$, which also play a role in estimating how the error in measurements of resonance frequencies propagates into the error in inverted material parameters. From Eq. (8) one can see that the less sensitive $f_n$ is to the change in $C_r$, the less accurate is the inversion of $C_R$ (and $Q_r^{-1}$) from resonance measurements. In extreme cases sensitivities of all resonance frequencies to some material parameters could be zero or simply too small for this parameter to be inverted, and it must be measured by some other means. Detailed error analysis of such a problem can be found elsewhere [12].

For isotropic carbon foams whose elastic properties are controlled by two independent Lame constants $\lambda$ and $\mu$, $2\mathbf{S}_{n\mu}$ is of the order of one for all $f_n(\mathbf{C}_r)$, while $2S_{N\lambda}$ does not exceed 0.1. Therefore, as it will be seen, separation of losses on $Q_r^{-1}$ and $Q_\lambda^{-1}$ is not attainable. Correspondingly, the specific damping capacity, $\Psi \approx 2\pi Q^{-1}$ [13], which is a normalized measure of total energy losses per cycle, is a more appropriate measure of material damping. Nevertheless, an explicit solution of Eq. (4) as well as it's inversion for $\mathbf{C}_{ijkl}$ is desirable to identify normal-mode resonances, estimate stress distribution in the sample material, and locate, albeit approximately, vibration nodes on the sample surface.

To solve the problem for an inhomogeneous sample one needs to make measurements at an infinite number of resonance frequencies. However, averaged elastic and loss constants can be

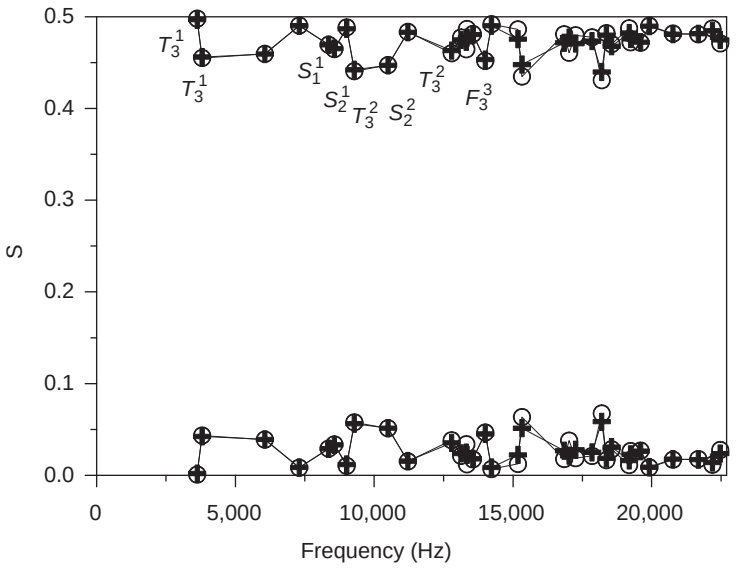


Fig. 1. Sensitivities $S_{n\mu}$ (upper curve) and $S_{n\lambda}$ (upper curve) for the 20 lowest natural-modes for homogeneous, (+), and inhomogeneous, (o), rectangular samples.

inverted, provided that the solution above is stable, that is a variation of sample density and/or elastic constants produces relatively small changes in resonance frequencies. As an example, $S_{n\mu}$ and $S_{n\lambda}$ for a sample with density distribution given by

$$\rho = \rho_0\left(1 + \exp\left(-3\left(\left(\frac{x_1}{L_1} - 0.75\right)^2 + \left(\frac{x_2}{L_2} - 0.75\right)^2 + \left(\frac{x_3}{L_3} - 0.75\right)^2\right)\right)\right) \tag{10}$$

for the 20 lower normal modes are presented in Fig. 1. Note the different scales for $S_{n\mu}$ and $S_{n\lambda}$ in the figure. As can be seen from Fig. 1 , $S_{n\mu}$ does not change significantly even though there is a 100% density increase at one of the corners of a sample. Correspondingly, for carbon foam, which exhibits a highly uniform micro-cellular distribution [2], the influence of inhomogeneity of its material properties has been ignored.

## 3. Experimental set-up

Rectangular, 128 mm × 75 mm × 32 mm samples of carbon foam (C-foam CF17 and CF25 [13]) have been used. Samples have densities of about 300 kg/m$^3$ for CF17 and 500 kg/m$^3$ for CF25 and pore sizes of 0.8 and 0.4 mm, correspondingly. A 10 mm diameter, 25 μm thick, copper foil was attached near the corner of the foam sample. Inductive current has been induced in the copper foil by an alternating magnetic field of appropriate frequency. Sample vibrations were excited by interaction of this current with a constant magnetic field produced by a small electromagnet. During decay measurements, the magnetic field (both alternating and constant

components) was turned off, thus avoiding possible additional damping caused by inductive currents in the foil or sample. The sample, the actuator, and the sample suspension were placed in a vacuum chamber at $10^3$ Pa. Sample vibrations were detected using a non-contact Laser vibrometer through the glass window in the wall of the vacuum chamber (see Fig. 2). Thus, excitation losses and sound radiation losses were excluded.

The output signal from the laser vibrometer was digitized with a 16-bit resolution and time dependence of the signal amplitude and hence the logarithmic decrement $q_n^e$ has been measured at the resonance frequency $f_n^{(e)}$ with the help of a sliding window fast Fourier transform (FFT) routine. The window width, $T$, was chosen to be equal to 16 periods of $f_n^e$, which is much less than the characteristic time-decay of the vibration system, $1/\Delta f_n^e$, but long enough to significantly improve the signal-to-noise ratio.

The difference made by support placement on the $q_n^{(e)}$ was used to estimate the support losses. In Ref. [14], it was experimentally found that simple suspension of a sample using two 0.1 mm diameter natural silk threads causes lower parasitic damping than other support material such as monofilament plastic wires, metal wire, and synthetic and natural fibre threads. An experiment has been carried out using a rectangular aluminium sample of the same width and length as typical carbon foam sample, which has about the same resonance frequency of the lowest frequency mode (sample mass was 0.341 kg). The supports were placed at the nodes and at the antinodes of the sample. The measured quality factors were $Q_{Aln} = 37000 \pm 5\%$ and $Q_{Alan} = 25000 \pm 10\%$ at the first flexural mode at 4.257 KHz, correspondingly. In this case, the higher data scatter for supports at antinodes is due to low repeatability of the measurements. Correspondingly, the maximum losses introduced by the supporting wires are around $(Q_{Alan}^{-1} - Q_{Aln}^{-1}) = 2 \times 10^{-5}$. The energy dissipated by supporting wires must be even smaller for lighter carbon samples while the stored kinetic energy is proportional to the mass of the sample. Therefore, the highest possible support losses for carbon samples should be of the order of $5 \times 10^{-5}$, which, as it will be seen, must be small (of the order of $10^{-2}$) compared to material losses in carbon foam samples. However, a significant difference (within $\pm 10\%$) between the measured quality factors has been found for samples supported at nodes and antinodes, which exceeds estimates made with aluminium samples, probably due to higher friction between the foam and

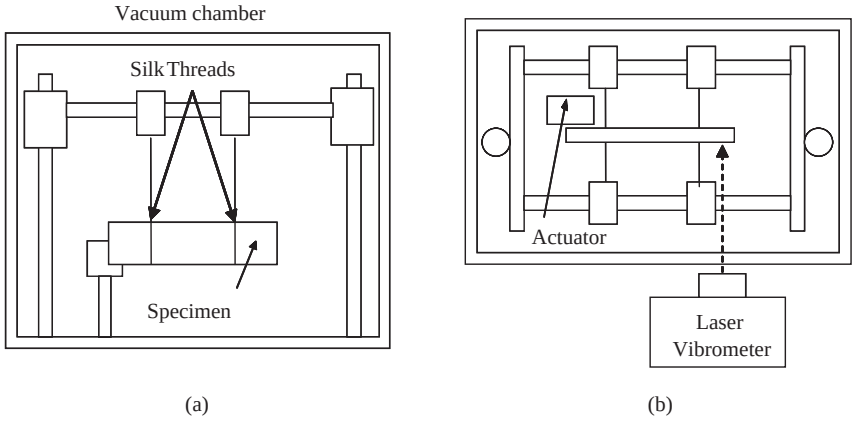


Fig. 2. Experimental set-up. (a) front view, (b) top view.

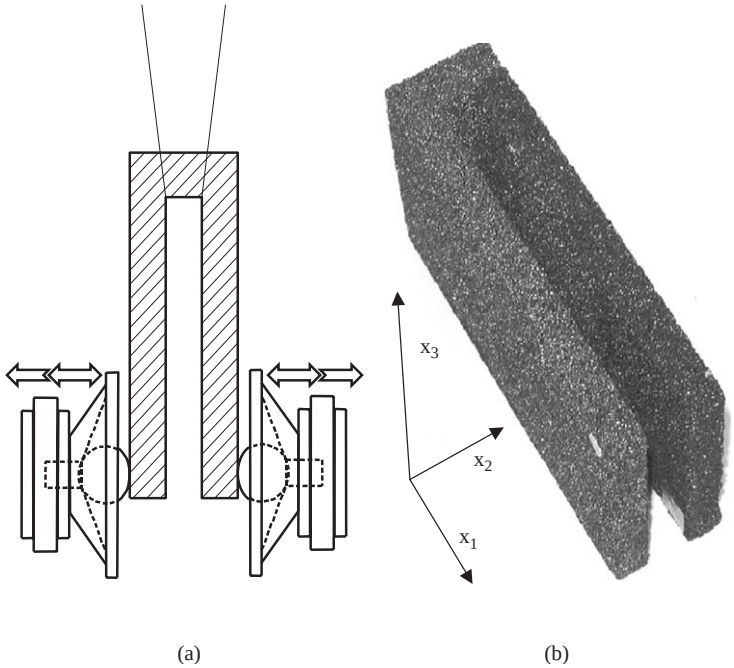


Fig. 3. Experimental set-up for low frequency wide dynamic range measurements: (a) Schematic of sample support and excitation; (b) photo of the tuning fork sample.

the supporting threads. Vibration amplitudes at the nodes of carbon samples were experimentally measured by scanning the sample surface with a laser vibrometer and found to be at least an order less than those at the antinodes. Correspondingly, the systematic error in damping measurements due to supports, if they are placed close to node positions, can be conservatively estimated to be of the order of a few per cent.

Two tuning fork samples have been carved from two 128 mm × 75 mm × 32 mm, CF17 samples using a high-speed diamond wheel by cutting a single 116 mm deep 12 mm wide cut in the middle of 75 mm × 32 mm edge along the 75 mm side. Additionally, one tuning fork has been made in similar fashion from the longer 200 mm × 36 mm × 40 mm, CF17 sample. To measure amplitude dependence of the specific damping, the first flexure mode was excited by two loudspeakers with voice coils in direct contact with opposite fork legs (see Fig. 3). After about 1000 cycles, the voice systems of loudspeakers were moved out of contact with the sample by passing a large constant current through them, and decay measurements were performed the way it has been done for rectangular-shaped samples.

## 4. Results and discussion

Five CF17 and five CF25 rectangular samples were tested. Their densities, dynamic shear modulus, specific damping capacity, $\Psi$, corresponding to maximum measured quality factor, and

Table 2
Specific damping capacity of carbon foam

| Sample name | Density, $\rho$ (kg/m$^3$) | Dynamic shear modulus, $\mu$ (Gpa) | Specific damping capacity, $\Psi \times 10^{-3}$ | Material damping, $Q_{\mu}^{-1} \times 10^{-3}$ |
|---|---|---|---|---|
| CF17-9 | 299.8 | 0.523 | 3.8 + 40% | 0.72 |
| CF17-7 | 304.9 | 0.533 | 3.4 + 40% | 0.67 |
| CF17-0 | 306.4 | 0.535 | 4.2 + 40% | 0.84 |
| CF17-6 | 314.1 | 0.497 | 3.6 + 40% | 0.67 |
| CF17-8 | 315.7 | 0.563 | 3.6 + 40% | 0.70 |
| CF25-4 | 484.8 | 0.944 | 11.4 + 50% | 2.39 |
| CF25-3 | 488.0 | 0.974 | 12.6 + 40% | 2.27 |
| CF25-1 | 508.5 | 1.040 | 9.8 + 40% | 2.1 |
| CF25-5 | 512.0 | 1.029 | 9.4 + 40% | 1.8 |
| CF25-2 | 530.2 | 1.032 | 10.8 + 40% | 2.1 |

internal material damping associated with shear modulus measured as an average for first eight normal modes are presented in Table 2. Normal modes, which have large displacement amplitudes normal to sample surface at the place of the actuator (the corner of the largest face a sample), were used (those are marked in Fig. 1). Ten tests were conducted for each sample. Repeatability of damping measurements for the same sample taken out of support and placed back was within 5% for all samples tested. As a means of calibration, elastic constants for Al6063 aluminium alloy were measured and were found to be $\lambda = 55.6$ GPa and $\mu = 26.56$ Gpa, which are very close to their table values.

There is, however, a significant scatter of data between samples of the same material and a significant difference between measured quality factors for different normal modes (the maximum observed scattering of $\Psi$ measurements for each specimen is presented in Table 2). As an example of frequency dependence of specific damping capacity, $\Psi$, for the two samples, namely CF17-0 and CF25-1, is presented in Fig. 4. Mode shapes are designated as $T$, $S$ and $F$ for torsion, shear and flexure correspondingly. The lower index corresponds to sample orientation, the upper index to harmonic order. Dashed lines represent inverted material damping, $Q_{\mu}^{-1}$ (multiplied by $2\pi$ to have direct comparison with $\Psi$). Larger scatter of data for higher modes can be explained by the possible influence of material inhomogeneity and/or unpredictable interaction of the foam with the supporting threads at higher vibration modes, when sample surface displacement magnitude sharply varies along the contact of sample surface with supporting threads. In addition to material damping, material inhomogeneity can cause vibration mode coupling, and an excitation of higher vibration modes. However, a spectral analysis of normal mode vibration shows that the ratio of magnitude of fundamental harmonic (at excitation frequency) to magnitude of any other normal mode exceeds 50 dB in all measurements (see Fig. 5). Corresponding additional damping is of the order of $10^{-5}$, which is small as compared to measured $Q_{\mu}^{-1}$. Higher density CF25 samples show much (three times) higher damping than lower density CF17 samples, contrary to what is expected if there is measurement error due to support losses [3]. It should be noted that although samples were manufactured using the same technological process, the foam manufacturer, Touch Stone

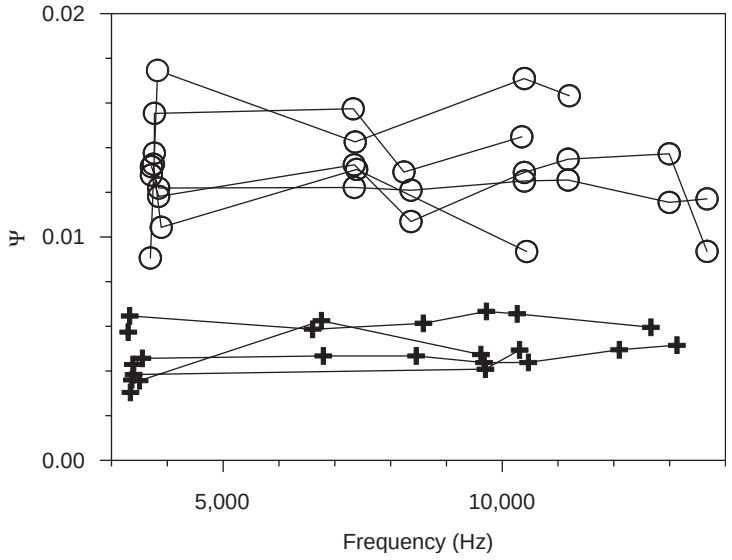


Fig. 4. Specific damping capacity of CF17 (+) and CF25 (o), carbon foam as a function of frequency.

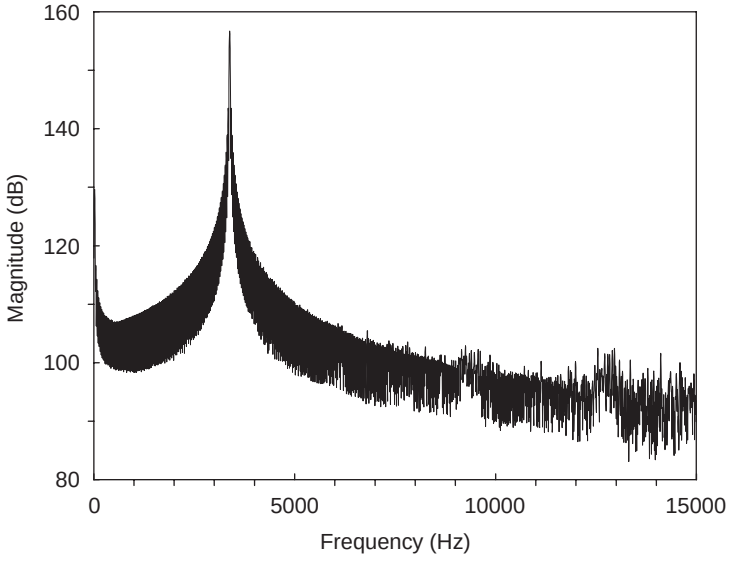


Fig. 5. Spectral purity of the $F_1^1$ mode.

Research Laboratory, uses raw material (coal) from different sources to manufacture CF17 and CF25 foams. That can explain the difference in material properties of foams of different density.

Analysis of the decay of the flexure mode of a tuning fork sample shows that specific damping capacity changes from $15 \times 10^{-3}$ to $5 \times 10^{-3}$ when vibration amplitude drops from 0.3 to $10^{-4}$ mm

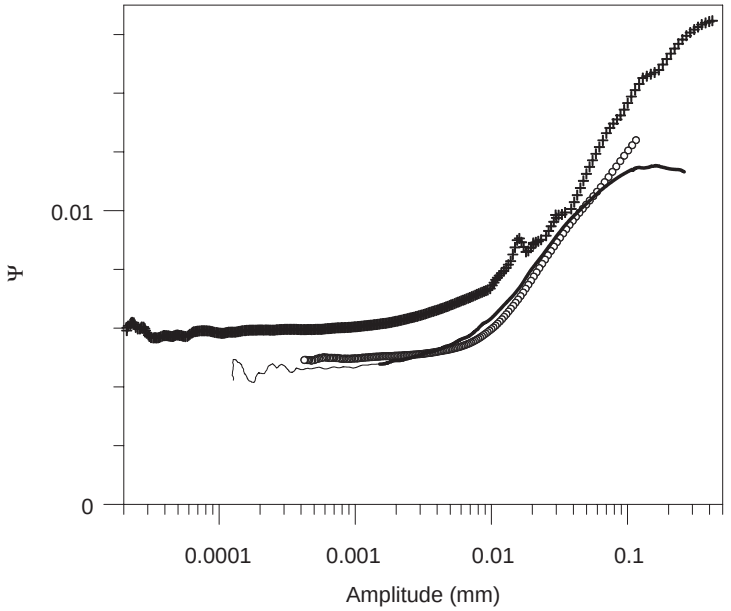


Fig. 6. Specific damping capacity of carbon foam as a function of vibration magnitude for CF17-1, (−), CF17-2, (o), and CF17-3, (+), samples.

(see Fig. 6). Resonance frequencies for CF17-1, CF17-2, CF17-3 samples were 112.6, 239.1 and 205.13 Hz, correspondingly. Maximum stress calculated from eigenvector solution (13) for the basis function set (15,16) is as follows: $\sigma_{12} = 0.7$ MPa, $\sigma_{11} = 1.2$ MPa, $\sigma_{22} = 0.9$ MPa. This is not very far from the ultimate tensile stress of 1.7 MPa and shear strength of 1.4 MPa given by the foam manufacturer. The significant increase in specific damping at a high stress level cannot be explained by nonlinearity because the relative change in free vibration frequency with decay of vibration magnitude did not exceed $10^{-5}$. The type of behaviour shown in Fig. 6 can be explained by dry friction between ligaments at high vibration amplitudes. This is, however, merely a conjecture and additional research at microscopic level is required to find the mechanism of additional damping at high vibration magnitudes.

## 5. Conclusion

(1) Simple and robust procedure of measurements for dynamic moduli and specific damping capacity in low damping foams has been developed. (2) In most cases no special sample preparation is required. (3) Carbon foam is shown to have moderate specific damping capacity of around $5 \times 10^{-3}$, which is constant in frequency ranges from 100 Hz to 20 KHz. (4) Specific damping capacity increases 2.5 times with magnitude of material deformation. (5) Specific damping capacity strongly depends on foam density changing from $4 \times 10^{-3}$ for CF17 foam to $4 \times 10^{-3}$ for CF25 foam, probably due to change in material damping caused by variation of the manufacturing process.

## Acknowledgements

Work has been supported by Air Force Grant PRDA-00-04-MLKN and Touch Stone Research Laboratory, Triadelphia, VA.

## References

[1] D.P. Anderson, K.M. Kearns, J.W. Klett, A.K. Roy, Microcellular graphitic carbon foams for next generation structures and thermal management, *Proceedings of the IEEE Aerospace Conference*, vol. 4, Big Sky, MT, USA, 2000, pp. 193–199.
[2] S. Ashley, Carbon foam for aerospace structures, *Mechanical Engineering* 119 (5) (1997) 28–29.
[3] J. Zhang, M.N. Gungor, E.J. Lavernia, Effect of porosity on the microstructural damping response of 6061 aluminium alloy, *Journal of Materials Science* 28 (1993) 1515–1524.
[4] J. Banhart, J. Baumeister, M. Weber, Damping properties of aluminum foams, *Material Science Engineering A* 205 (1996) 221–228.
[5] G. Lu, G.Q. (Max) Lu, Z.M. Xiao, Mechanical properties of porous materials, *Journal of Porous Materials* 6 (1999) 359–368.
[6] W.M. Visscher, A. Migliori, T.M. Bell, R.A. Reinert, On the normal modes of free vibration of inhomogeneous and anisotropic elastic objects, *Journal of the Acoustical Society of America* 90 (1991) 2154–2162.
[7] T. Kant, K. Swaminathan, Free vibration of isotropic, orthotropic, and multilayer plates based on higher order refined theories, *Journal of Sound and Vibration* 241 (2001) 319–327.
[8] R.K. Singh, H.A. Smith, Comparison of computational effectiveness of the finite element formulations in free vibration analyses, *Computers and Structures* 51 (1994) 381–391.
[9] H.H. Demarest Jr., Cube-resonance method to determine the elastic constants of solids, *Journal of the Acoustical Society of America* 49 (1971) 768–775.
[10] I. Ohno, Free vibration of a rectangular parallelepiped crystal and its application to determination of elastic constants of orthorhombic crystals, *Journal of Physics of the Earth* 24 (1976) 355–379.
[11] Y. Sumino, I. Ohno, T. Goto, M. Kumazawa, Measurement of elastic constants and internal frictions on single-crystal MgO by rectangular parallelepiped resonance, *Journal of Physics of Earth* 24 (1976) 263–273.
[12] C.L. Yapura, V.K. Kinra, K. Maslov, Measurement of six acoustical properties of a three-layered medium using resonant frequencies, *Journal of the Acoustical Society of America* 115 (2004) 57–65.
[13] D.K. Rogers, J. Plucinski, P.G. Stansberry, A.H. Stiller, J. W. Zondlo, Low-cost carbon foams for thermal protection and reinforcement applications, *Proceedings of the International SAMPE Symposium Exhibition*, vol. 45(1), Long Beach, USA, 2000, pp. 293–307.
[14] G.G. Wren, V.K. Kinra, An experimental technique for determining a measure of structural damping, *Journal of Testing and Evaluation* 16 (1988) 77–85.